SYNTHESIS AND CHARACTERIZATION OF MAGNETITE NANOPARTICLES COATED WITH FOLIC ACID AS TARGETED MRI CONTRAST AGENTS

A. KHORRAMDOUST [a], M. ASHOOR [a*], K. SABERYAN [b], A. EIDI [a]
[a]Department of Biology, Science and Research Branch, Islamic Azad University, Tehran, Iran
[b]Nuclear Materials and Fuel Cycle Research School, Nuclear Science and Technology Research Institute, AEOI, P.O. Box: 11365-8486, Tehran, Iran

Perception the process of synthesis of magnetic nanoparticles is important for its performance in in vitro and in vivo process. In this work we report the synthesis of magnetic nanoparticles with co-precipitation chemical method. The nanostructured material was coated with Folic acid and dispersed in aqueous medium. The X-ray diffraction (XRD) studies and the transmission electron microscopy (TEM) images showed that the synthesized magnetite particles had 9 nm dimensions. For ensuring the availability of Folic acid on nanoparticles, Fourier transform infrared spectroscopy (FT-IR) was used. Furthermore, magnetic properties of the products were studied by vibrating sample magnetometer (VSM).

1. Introduction

Magnetic Resonance Imaging (MRI) has been widely used as a primary medical imaging technique in radiology to visualize the internal structure and function of the body in which the MRI contrast agents are used to improve sensitivity and diagnostic confidence [1]. Contrast agents incorporating superparamagnetic iron-oxide nanoparticles have shown promise as a means to visualize labeled cells using MRI. Labeled cells cause significant signal dephasing due to the magnetic field in homogeneity induced in water molecules near the cell. With the resulting signal void as the means for detection, the particles behave as a negative contrast agent, which can suffer from partial-volume effects [2]. Magnetite (Fe_3O_4) is a kind of mixed iron oxide ($FeO \cdot Fe_2O_3$) with an inverse spinel crystal structure in this structure, half of the Fe^{3+} ions are tetrahedrally coordinated while the other half of the Fe^{3+} ions and all of the Fe^{2+} ions are octahedrally coordinated. Each octahedral site has six nearest neighbor O^{2-} ions arranged on the corners of an octahedron; meanwhile, each tetrahedral site has four nearest neighbor O^{2-} ions arranged on the corners of a tetrahedron [3]. Fe_3O_4 nanoparticles equal tumor cell membranes has negatively charged, which affects tumor cell uptake of Fe_3O_4 nanoparticles. The naked Fe_3O_4 nanoparticles cannot effectively label tumor cells. To achieve an effective labeling of magnetic nanoparticles on tumor cells, the optimal method is to couple magnetic nanoparticles to specific targeting molecules which have high affinity with the target tumor cells [4, 5]. Many specific targeting molecular markers for the tumor cells were mentioned in many reports [6-10]. However, some agents are expensive and anti-body molecules are too big and hinder the crossing of the coupled magnetic nanoparticles through biological barriers [11]. Folic acid or folate (pteroylglutamate) is water-soluble and is brought into both healthy and cancerous cells by the folate-receptor. This receptor is used to transport folate into the cytosol for the synthesis of thymine by dihydrofolate reductase. The presence of the folate-receptor on a cell's surface is regulated by the cell's function. Cancer cells tend to overexpress the folate-receptor because of their vast requirement for folate. It has

---

* Corresponding author: mashoor@aeoi.org.ir

been proposed that the folate-receptor makes for a suitable targeting agent because of its relatively low expression level in healthy tissues and overexpression in cancerous tissues [12].

In order for SPIONs to be effective MRI contrast agents, they must be able to evade body's immune system in order to minimize their premature clearance from the blood stream. There are two main pathways through which SPIONs may be prematurely removed from circulation, either via uptake by the reticulo-endothelial system (RES), or through renal clearance mechanisms. The hydrodynamic size of the particles is a primary factor in determining which clearance pathway will be followed. Particles greater than 200 nm are generally cleared via the RES [13, 14]. The particles with a hydrodynamic diameter of less than 5.5 nm (± 10 %) are removed through renal filtration [15]. In general, particles between 10 and 100 nm in diameter have the greatest circulation time; their reduced surface area, compared to large SPIONs, minimizes the space available for adsorption of RES proteins, yet they are still large enough to evade renal clearance [16-18]. Jun et al. has reported that the superparamagnetic SPIONs exhibit a high magnetization when an external magnetic field is applied; the magnetization becomes zero when the external magnetic field is removed. They provide the negative (dark) contrast by enhancing T_2 (T_2*) relaxivity of water protons for MRI [19]. Lartigue et al. has reported that the folate surface of maghemite NPs could recognize the folate receptor and was proven by folate receptor expressing cell lines or by radio-labeled folic acid in competitive binding experiments. Water-dispersible sugar-coated SPIONs were designed as magnetic fluid hyperthermia heat mediators and T_2 negative contrast agents for MRI [20]. Zhou et al. were synthesized by a non-solvent-aided coacervation procedure followed by a chemical cross linking procedure. The surfaces of CS-coated Fe_3O_4 NPs were successfully functionalized with folate-poly (ethylene glycol)-COOH (FA-PEG) to obtain novel FA-PEG-CS-coated Fe_3O_4 NPs endowed with long blood circulation and specific targeting capacity [21]. Barick et al. were synthesized folate-conjugated luminescent iron oxide nanoparticles and has reported that these FLIONs show good colloidal stability, high magnetic field responsivity and excellent self-heating efficacy. Specifically, a new class of magnetic nanoparticles has been fabricated, which can be used as an effective heating source for hyperthermia [22]. Chen et al. were synthesized magnetic Fe_3O_4 nanoparticles and checked their cytotoxic effect on the human breast adenocarcinoma cell line (MCF-7) cells; he has demonstrated that the Fe_3O_4 nanoparticles had no effect on the main organs and blood biochemistry in a rabbit model. MTT and flow cytometry assays revealed that Fe_3O_4 nano magneto fluid thermotherapy inhibited MCF-7 cell proliferation, and its inhibitory effect was dose-dependent according to the Fe_3O_4 nano magneto fluid concentration [23].

In this study, we intent to synthesize folic acid-coated Fe_3O_4 NPs of 9 nm particle size, which exhibits excellent magnetic properties, and can be useful as a contrast agent in MR imaging, by using hydrolysis followed by co-precipitation of the corresponding metal (Fe^{3+} and Fe^{2+}) salts. Further, we platform to characterize the physical and magnetic properties of these synthesized nanoparticles as well as its rudimentary application as MR contrast agent for various in vitro and in vivo systems.

2. Experimental section

2.1. Materials
All chemicals including $FeCl_2.4H_2O$, $FeCl_3.6H_2O$, NaOH, Folic acid with analytical grade were supplied from Merck Company and were used without further purification and used Ethanol, Distilled water and Argon gas.

2.2. Synthesis of Fe₃O4 coated with Folic acid
Dissolved $FeCl_3·6H_2O$ and $FeCl_2·4H_2O$ (mole ratio 2:1) in deionized water under Argon with mechanical stirring at 1000 rpm (revolution per minute) and added NaOH 2M Gradually. With another burette added Folic acid (that is dissolved in water with a drop of NaOH is alkaline) progressively. During the reaction process, the pH was maintained at about 9. The precipitates were washed several times with deionized water and ethanol. Finally, they were dried in a vacuum oven at 60°C.

2.3. Characterization of MNPs
2.3.1 X-Ray Diffraction (XRD)

XRD experiments of the crystalline phase of a powder sample of MNPs were performed using an X-ray diffractometer (STADI-MP, STOE Company, with monochromatized Cu Kα radiation). The parameters of the measurements were: 40 kV and 30 mA, angular variation range 5 to 100° in steps of 0.05° for each 10 s (geometry $\theta - 2\theta$).

2.3.2. Transmission Electron Microscopy (TEM)

The morphology of the MNPs in the colloidal suspension was observed with a Leo 906E (Zeiss) TEM microscope at 100 kV. A drop of the colloidal suspension (100 μg Fe/mL) was dispersed and dried on a copper grid covered with collodion and carbon prior to the experiment.

2.3.3. Magnetic Measurements by VSM

Magnetic measurements were carried out with a vibrating sample magnetometer (VSM).

2.3.4. FT-IR spectrum

Fourier transform infrared spectroscopy (FT-IR) method (Bruker Vector 22 model) was used for functional groups investigations in the range of 4000-400 cm^{-1}.

3. Results

3.1 XRD analysis for MNPs

Fig. 1 shows the XRD pattern of the synthesized MNPs, which was quite identical to Fe_3O_4 MNPs coated with Folic acid and indicating that the sample has a cubic crystal system. Also, we can see that no characteristic peaks of impurities were observed. The average MNPs sizes calculated about 9 nm using Scherer formula.
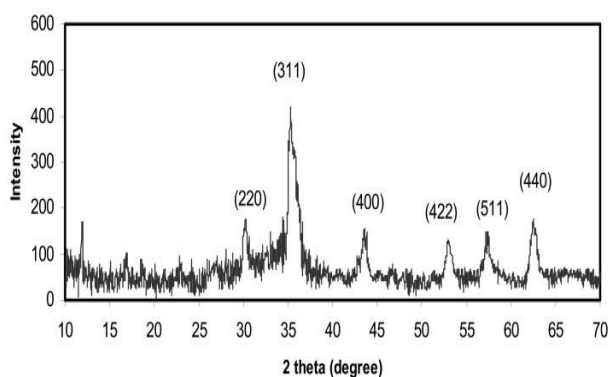
Fig. 1. XRD pattern of Fe_3O_4 MNPs coated with Folic acid

The characteristic peaks of Fe_3O_4 MNPs coated with Folic acid at $2\theta = 30.1°$, $35.4°$, $43.9°$, $54.4°$, $57.0°$, $63.6°$ and $74.0°$, marked by their indices ((2 2 0), (3 1 1), (4 0 0), (4 2 2), (5 1 1), (4 4 0) and (533)), which accorded well with the database (JCPDS 01-1111) were observed for synthesis of magnetite nanoparticles confirming the presence of the crystalline structure of the magnetite.

3.2 FT-IR analysis for MNPs

Fig. 2 shows the functional groups of amine-functionalized magnetite nanoparticles were identified using FT-IR. Furthermore, the molecular formula and 2D structure of Folic acid were indicated in Figs. 3 and 4, respectively.
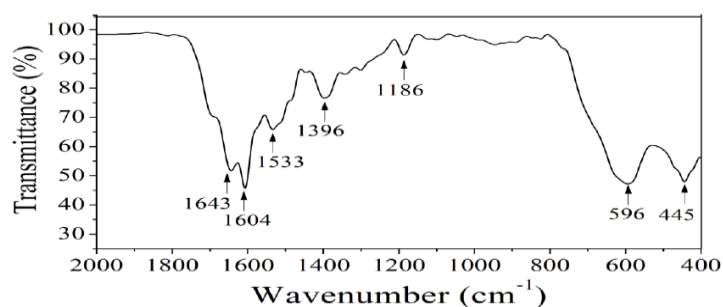
Fig. 2. FT-IR spectrum of Fe$_3$O$_4$ Coated with Folic acid
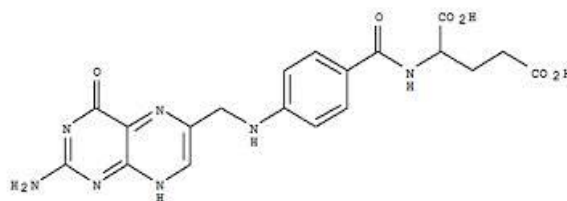
Fig. 3. Molecular Formula of Folic acid: C$_{19}$H$_{19}$N$_7$O$_6$
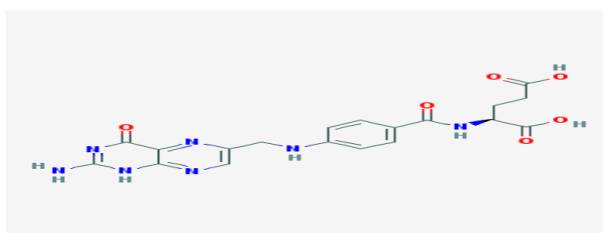
Fig. 4. 2D structure of Folic acid

The absorption peaks at 596 cm^{-1} and 445 cm^{-1} are attributed to Fe-O bond absorption. Absorption at 1643 cm^{-1} can be attributed to N-H bending vibration, which is also favorable evidence for the existence of primary amine in molecules. Absorption at 1604 cm^{-1} corresponded to the aromatic ring stretching vibration in the folic acid molecule, absorption at 1396 cm^{-1} corresponded to the benzoic.

3.3 TEM analysis for MNPs

Fig. 5 illustrates the TEM photograph of MNPs. It is seen that most nanoparticles exhibit spherical, cubic shapes and have particle size of about 9 nm. Thus, the MNPs were well prepared in nano-size via the chemical co-precipitation method employed in this study. The Folic acid coated on the nanoparticles resulted in its hydrophilic property.
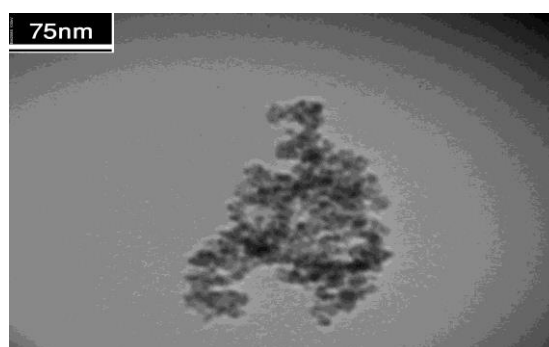
Fig. 5. TEM photograph of Fe$_3$O$_4$ Coated with Folic acid

3.4 VSM analysis for MNPs

The saturation magnetization value of the hydrophilic magnetite nanoparticles was 23 emu/g measured by VSM, as shown in Fig. 6.
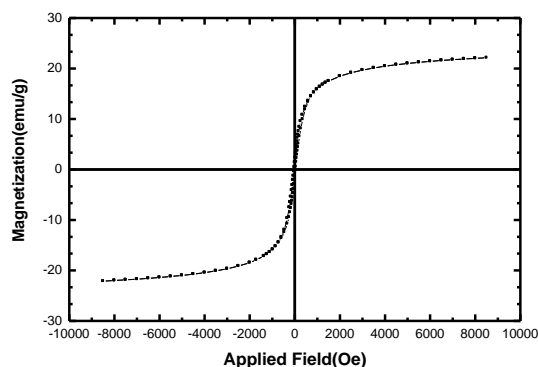
Fig. 6. VSM of Fe$_3$O$_4$ Coated with Folic acid

4. Discussion

The folic acid receptor appears to be a promising target for cancer imaging and treatment. Folic acid receptors are highly overexpressed on the surface of many tumor types. This expression can be exploited to target therapeutic compounds directly to cancerous tissues using many avenues. While these studies synthesis of magnetite nanoparticles coated with Folic acid, the use of folic acid as targeted MRI contrast agents. Many works need to be done to find the correct dosages and potential long-term effects of nanoparticle drug delivery for MRI contrast agents. Also, in countries that fortify foods with folic acid, or in people who take folic acid supplements, interactions between the effects of folic acid and antifolic acid need to be explored. Nevertheless, the successful use of folic acid conjugates indicates that receptor targeted nanoparticle as targeted MRI contrast agents.

5. Conclusions

The development of MNPs has been greatly accelerated in the past decade by advances in nanotechnology, molecular cell biology, and small-animal imaging instrumentation. MNPs of various formulations have been developed to diagnose and treat diseases for which conventional therapy has shown limited efficacy. In particular, the use of MNPs as MRI contrast agents and drug carriers has drawn enormous attention, as it holds great potential of providing new opportunities for early cancer detection and targeted therapies. This technology will not only minimize invasive procedures, but also reduce side effects to healthy tissues, which are two primary concerns in conventional cancer therapies. Improving imaging contrast, biocompatibility, and specific targeting capability remains the mainstay of MNP development for medicine. To improve MRI signal-to-background ratios, MNP cores with high magnetic moments, such as doped iron oxide nanocrystals, metallic/alloy nanoparticles, and nanocomposites, have been developed. To improve biocompatibility, surface coatings, such as gold, silica and a number of biocompatible polymers have been investigated. The use of gold or silica as shell materials allows for potential application of toxic materials as nanoparticle cores with strong magnetic properties. The conjugation of biocompatible polymers, such as dextran, PEG, or other protein resistant polymers, as surface coating for MNPs, prevents nanoparticles from aggregation and opsonization, evades nanoparticle uptake by the RES, and increases colloidal stability in physiological solutions and blood circulation time. Specific targeting capability is commonly achieved by conjugation of peptides, aptamers, and small biomolecules with high affinity to target cells, on the surface of MNPs, aimed to increase the local accumulation and retention of the MNPs in pathological sites while reducing side effects. Interestingly, some targeting agents, such as MTX and CTX, also

exhibit therapeutic effects for target cells, which allows the MNPs to serve multiple functions including diagnosis, treatment, and even treatment monitoring. It is worthwhile mentioning that such targeting agents are not common, and multifunctionality is usually achieved by conjugation of several agents. MNPs serving as multimodal imaging agents or multifunctional carriers are actively pursued. With continued advances in nanomaterials synthesis technology, surface chemistry, and knowledge in interactions of materials with biological systems, such a strategic approach is becoming a commonplace. Influence of folic acid in controlling the structural effects of Fe_3O_4 nanoparticle under physiological conditions of temperature and pH has been studied as a novel method. The physical investigations with XRD, TEM, FT-IR and VSM tools have been carried out in order to understand the interesting structural changes involved in the system which may find important biomedical applications. Photo induced charge transfer due to folic acid ensconced Fe_3O_4 nanoparticle is particularly a noticeable effect as seen from our results.

Acknowledgements

References

[1] K. N. Raymond, V. C. Pierre, Bioconjug Chem, **16**(1): 3-8 (2005).

[2]C. H. Cunningham, T. Arai, P. C. Yang, M. V. McConnell, J. M. Pauly, and S. M. Conolly, Magn Reson Med **53**: 999–1005 (2005).

[3] R. C. O'Handley, Principles and Applications, John Wiley & Sons, New York, p. 126 (2000)

[4] R. Weissleder, A. Bogdanov, Magn Reson Q, **8**(1): 55−63 (1992).

[5] Y. M. Huh, Y. W. Jun, H. T. Song, S. Kim, J. S. Choi, J. H. Lee, S. Yoon, K. S. Kim, J. S. Shin, J. S. Suh, J. Cheon, J Am Chem Soc, **127**: 12387−12391 (2005).

[6] K. L. Hultman, J. A. Raffo, A. L. Grzenda, P. E. Harris, T. R. Brown, S. O'BRIEN, Acs Nano, **2**(3): 477−484 (2008).

[7] B. Feng, R. Y. Hong, L. S. Wang, L. Guo, H. Z. LI, J. DING, Y. Zheng, D. G. Wei, Colloids and Surfaces A: Physicochem Eng Aspects, **328**: 52−59 (2008).

[8] W. H. Chen, P. W. Yi, Y. Zhang, L. M. Zhang, Z. W. Deng, Z. J. Zhang, Appl Mater Interfaces, **3**: 4085−4091 (2011).

[9] I. Garcia, J. Gallo, N.Genicio, D. Padro, S. Pecades, Bioconjugate Chem, **22**: 264−273 (2011)

[10] E. Poselt, C. Schmidtke, S. Fischer, K. Peldschus, J. Salamon, H. Kloust, H. Tran, A. Pietsch, M. Heine, G. Adam, U. Schumacher, C. Wagener, S. Forester, H. Weller, Acs Nano, **6**(4): 3346-3355 (2012).

[11] S. E. Mcneil, J Leukoc Biol, **78**: 585−594 (2005).

[12] G. A. Mansoori, S. K. S. Brandenburg, A. Shakeri-Zadeh, Cancers, **2**: 1911-1928 (2010).

[13] A. K. Gupta, M. Gupta, Biomaterials. **26**: 3995-4021 (2005).

[14] S. Laurent, D. Forge, M. Port, A. Roch, C. Robic, L. V. Elst, et al, Chem Rev. **108**: 2064-110 (2008)

[15] H. S. Choi, W. Liu, P. Misra, E. Tanaka, J. P. Zimmer, B. I. Ipe, Nat Biotechnol. **25**: 1165-70 (2007)

[16] Y. J. Wang, S. M. Hussain, G. P. Krestin, Eur Radiol. **11**: 2319-31 (2001)

[17] T. Neuberger, B. Schopf, H. Hofmann, M. Hofmann, B. V. Rechenberg, J Magn Magn Mater. **293**: 483-96 (2005)

[18] L. Brannon-Peppas, J. O. Blanchette, Adv Drug Deliv Rev. **56**: 1649-59 (2004)

[19] Y. W. Jun, J. W. Seo, J. Cheon, Acc. Chem. Res. **41**: 179-89 (2008)

[20] L. Lartigue, C. Innocenti, T. Kalaivani, A. Awwad, M. Duque, Y. Guari, J. Larionova, C. Guérin, J-L. G. Montero, V. Barragan-Montero, P. Arosio, A. Lascialfari, D. Gatteschi, C. Sangregorio, J. Am. Chem. Soc. **133**: 10459-72 (2011)

[21] S. Zhou, Y. Li, F. Cui, M. Jia, X. Yang, Y. Wang, L. Xie Q. Zhang, Z. Hou, Macromolecular Research. January, **22**(1): 58-66 (2014)

[22] K. C. Barick, S. Rana, P. A. Hassan, AIP Conference Proceedings; **1591**: 561 (2014).
[23] D. Chen, Q. Tang, X. Li, X. Zhou, J. Zang, W. Xue, J. Y. Xiang, C. Q. Guo, Int J Nanomed. **7**: 4973–4982 (2012)